

Eradication of Multidrug-Resistant *Pseudomonas* Biofilm with Pulsed Electric Fields

Saiqa I. Khan,¹ Gaddi Blumrosen,² Daniela Vecchio,^{3,4} Alexander Golberg,^{5,6} Michael C. McCormack,¹ Martin L. Yarmush,^{5,7} Michael R. Hamblin,^{3,4,8} William G. Austen Jr¹

¹Division of Plastic and Reconstructive Surgery, Massachusetts General Hospital, Harvard Medical School, Boston, Massachusetts 02114; telephone: 617-726-6943; fax: 617-726-8998; e-mail: sikhan@mgh.harvard.edu, saiqakhan7@gmail.com

²Department of Computer Science, Tel Aviv University, Tel Aviv, Israel

³Wellman Center for Photomedicine, Massachusetts General Hospital, Boston, Massachusetts 02114

⁴Department of Dermatology, Harvard Medical School, Boston, Massachusetts 02115

⁵Center for Engineering in Medicine, Department of Surgery, Massachusetts General Hospital, Harvard Medical School, and the Shriners Burns Hospital, Boston, Massachusetts 02114

⁶Porter School of Environmental Studies, Tel Aviv University, Tel Aviv, Israel

⁷Department of Biomedical Engineering, Rutgers University, Piscataway, New Jersey 08854

⁸Harvard-MIT Division of Health Sciences and Technology, Cambridge, Massachusetts 02139

ABSTRACT: Biofilm formation is a significant problem, accounting for over eighty percent of microbial infections in the body. Biofilm eradication is problematic due to increased resistance to antibiotics and antimicrobials as compared to planktonic cells. The purpose of this study was to investigate the effect of Pulsed Electric Fields (PEF) on biofilm-infected mesh. Prolene mesh was infected with bioluminescent *Pseudomonas aeruginosa* and treated with PEF using a concentric electrode system to derive, in a single experiment, the critical electric field strength needed to kill bacteria. The effect of the electric field strength and the number of pulses (with a fixed pulse length duration and frequency) on bacterial eradication was investigated. For all experiments, biofilm formation and disruption were confirmed with bioluminescent imaging and Scanning Electron Microscopy (SEM). Computation and statistical methods were used to analyze treatment efficiency and to compare it to existing theoretical models. In all experiments 1500 V are applied through a central electrode, with pulse duration of 50 μ s, and pulse delivery frequency of 2 Hz. We found that the critical electric field strength (Ecr) needed to eradicate 100–80% of bacteria in the treated area was 121 ± 14 V/mm when 300 pulses were applied, and 235 ± 6.1 V/mm when 150 pulses were applied. The area at which 100–80% of bacteria were eradicated was 50.5 ± 9.9 mm² for 300 pulses, and 13.4 ± 0.65 mm² for 150 pulses. 80% threshold eradication was not achieved with 100 pulses. The

results indicate that increased efficacy of treatment is due to increased number of pulses delivered. In addition, we that showed the bacterial death rate as a function of the electrical field follows the statistical Weibull model for 150 and 300 pulses. We hypothesize that in the clinical setting, combining systemic antibacterial therapy with PEF will yield a synergistic effect leading to improved eradication of mesh infections.

Biotechnol. Bioeng. 2015;9999: 1–8.

© 2015 Wiley Periodicals, Inc.

KEYWORDS: biofilm; treatment of mesh infection; pulsed electric fields; medical device disinfection; eradication of multidrug resistant infections; irreversible electroporation

Gaddi Blumrosen and Daniela Vecchio contributed equally to this work.

Correspondence to: S.I. Khan

Contract grant sponsor: US NIH

Contract grant number: R01AI050875

Received 21 April 2015; Revision received 10 August 2015; Accepted 23 August 2015

Accepted manuscript online xx Month 2015;

Article first published online in Wiley Online Library (wileyonlinelibrary.com).

DOI 10.1002/bit.25818

Introduction

Mesh infection is an example of a type of implant infection where surgical removal and debridement can result in significant morbidity for patients. Two million Americans undergo abdominal surgery annually with a postoperative incisional hernia rate of 10–23 percent. About 400,000 ventral hernia repairs are performed each year in the United States alone, with reported hernia recurrences in 40–50 percent of cases. Synthetic mesh reinforces hernia repairs and has been shown to decrease recurrences compared to primary repair alone. However, morbidities related to mesh infection can limit efficacy. Reported mesh infection rates range from 4–16 percent (Albino et al., 2014). Known mesh complications include infection requiring prolonged antibiotic coverage, surgical debridements, and mesh explantation.

Postoperative mesh infections requiring debridement and mesh explantation continue to be devastating problems for patients and a reconstructive challenge for surgeons.

Synthetic mesh is currently the most common repair material used for reinforcement of ventral hernias. For this reason, prolene mesh was selected in this study. Multiple pathways may lead to infection of synthetic mesh. Patients may have an acute postoperative mesh infection, or dehiscence of the wound may expose the mesh, leading to colonization, and infection of the prosthesis. Reoperation through synthetic mesh may also lead to infection. Additionally, seromas that develop may become infected, leading to subsequent contamination, and removal of the prosthesis (Breuing et al., 2010).

Antibiotics alone are not an effective treatment for mesh infections. The bacteria that commonly infect mesh are *Methicillin-Resistant Staphylococcus aureus* (MRSA), *Enterococcus faecalis*, *Escherichia coli*, *Proteus mirabilis*, *Prevotella bivia*, and *Pseudomonas aeruginosa* (Albino et al., 2014). In this study, we showed that Pulsed Electric Fields (PEF) can disinfect the mesh from *P. aeruginosa* infection. *P. aeruginosa* is a Gram-negative rod measuring 1–5 μm long and 0.5–1.0 μm wide, containing one or more flagella. *P. aeruginosa* forms biofilms through producing and excreting exopolysaccharides (EPS) such as alginate, which makes it difficult for the bacteria to be phagocytosed by a patient's white blood cells. In vitro, *P. aeruginosa* biofilms consist of microcolonies encapsulated by EPS, in which the biofilm is comprised of water channels that function as a distribution system for oxygen and nutrients (Costerton et al., 1995). *P. aeruginosa* can form biofilms on virtually any surface under any environmental or nutritional conditions (Sandt et al., 2007). For the above reasons, the virulent *P. aeruginosa*, was selected as the target for this study.

The formation of biofilm is a significant medical problem, accounting for over eighty percent of microbial infections in the body (2002-12-20). Control of biofilm persistence and growth is problematic due to increased resistance to treatment with antibiotics as compared to planktonic cells (Davies and Marques, 2009). Bacterial infections that exist as single independent cells are referred to as planktonic, and are generally treated with antibiotics depending on fast and accurate diagnoses (Bjarnsholt, 2013). In contrast, a biofilm is an accumulation of microorganisms embedded in a polysaccharide matrix, which adheres to a biologic or non-biologic surface. The matrix of extracellular polymeric substances (EPSs) has an essential role in defining the cohesiveness and other physical properties of these adherent microbial communities (Xavier et al., 2005). Additionally, biofilm growth increases the opportunity for gene transfer between bacteria, therefore further perpetuating antibiotic resistance (2002-12-20).

Techniques for promoting biofilm detachment with chemical and enzymatic agents that attack the EPS matrix have been investigated with variable and overall disappointing results (Chen, 2000; Xavier et al., 2005). As there is no effective treatment for biofilm infections, the gold standard treatment is mechanical removal of the infected material and/or tissue. Mechanical removal is not always possible without risk of serious complications (Bjarnsholt, 2013). If the biofilm infected material cannot be removed, the patient is placed on chronic suppressive antibiotics, therefore requiring several different antibiotics at high doses for an extended period of time

(Hoiby et al., 2010). This may induce further resistance, tolerance, and eventually chronic infection (Jolivet-Gougeon et al., 2011).

Therefore, new non-antibiotic based interventions are needed to address biofilm infections and reduce emerging bacterial resistance to multiple drugs. Here we propose PEF as a novel, non-chemical, non-thermal tool to potentially eradicate biofilm on implanted medical devices. This PEF approach may avoid costly treatments such as reoperation to remove infected material, and reduce subsequent morbidity, recurrence, life-long high dose antibiotic regimens, and decreased quality of life.

High voltage, microsecond pulsed electric fields create non-thermal pores in cell membranes. This phenomenon is called electroporation. Electroporation based technologies are very attractive for various cell therapies. Electroporation can be reversible or irreversible (Yarmush et al., 2014). Reversible electroporation is commonly used for gene or drug delivery into cells (Golberg and Yarmush, 2013). Reversible electroporation has medical applications in electro-chemotherapy and gene-electrotherapy (Manca et al., 2013; Mir et al., 2006; Sersa et al., 2008) for the delivery of small molecules and genes to modify tissue function. Irreversible electroporation is created through the use of high voltage, short PEF which create non-thermal permanent damage to cell membranes. Irreversible electroporation is used for direct, non-thermal ablation of solid tumors (Neal et al., 2011): a procedure known as non-thermal irreversible electroporation (NT-IRE) (Golberg, 2013). In another application, intermittent delivery of PEF has been shown to provide long term control of bacterial contamination in pharmaceuticals and food (Golberg, 2015; Weaver, 2000).

Our group has previously used PEF for disinfection of murine burn wounds contaminated with antibiotic-resistant *Acinetobacter baumannii* (Golberg et al., 2014a,b). Now, we report on a method to optimize PEF for device/implant disinfection. Determination of electric fields parameters even in vivo is a tedious task, usually requiring multiple experiments. In this study, to test the effect of PEF for disinfection of synthetic mesh, we used a concentric ring configuration (Fernand et al., 2012) to determine the ideal electric field strength needed to eradicate bacteria and produce biofilm disruption. This specific configuration of concentric electrodes allows rapid testing of the effects of multiple electric fields in a single experiment. Subsequently, we investigated the effect of the electric field strength and number of pulses delivered, on bacterial survival and biofilm morphology in vitro, using a tissue phantom model of infected mesh embedded in agarose gel.

Although appreciated for four decades as an effective tool for bacterial disinfection in the food industry (Golberg et al., 2010), PEF technology has yet to be investigated in the treatment of prosthetic implant infections. This new application of PEF to biofilms provides a possible treatment for biofilm infections that avoids the morbidity and complications associated with removal of infected material and chronic high-dose antibiotics.

Methods

Bacterial Culture

Sterile nonabsorbable synthetic prolene mesh (Ethicon, CA) was infected with the pathogenic Gram-negative bacterium

Pseudomonas aeruginosa that had been rendered bioluminescent. The *P. aeruginosa* strain employed was ATCC 19660 (strain 180). It can cause septicemia by intraperitoneal injection (Rosenthal, 1967) and is pathogenic in mice with infected cutaneous burns (Markley and Smallman, 1968). The bioluminescent variant (strain Xen 05) carried the integrated bacterial *lux* operon into its chromosomes for stable bacterial luciferase expression, which allowed them to be used for bioluminescent imaging (Rocchetta et al., 2001) (strain Xen 05, kind donation from Xenogen Inc., Alameda, CA).

A colony of bioluminescent *Pseudomonas aeruginosa* was then placed in a 50 mL falcon tube with prolene mesh and 30 mL of brain heart infusion broth (BHI, purchased from Fisher). This was agitated on a shaker at 180 rpm for 30 min at room temperature and then moved to a C24 Incubator Shaker (Brunswick Scientific) at 37°C with agitation at 100 rpm for three days. After three days, the infected mesh were placed on sterile agar plates and incubated overnight at 37°C, 5% CO₂.

Single Step Determination of a Critical Local Electric Field Strength With Concentric Ring Electroporation

Concentric ring electroporation as described by Fernand et al. (2012) was used, which delivers a centrifugal gradient of disinfection from the center outwards to the periphery. The center of the mesh, where the needle is in direct contact, receives the highest electric field strength. This electric field strength, therefore, decreases in an outward direction from the center to the outer rim. For concentric ring electroporation, the following equation is used to solve for the local electric field strength $E(r)$ at any given radius (r). In the system of concentric electrodes, the field strength is a function of radius, and applied voltage (V) according to the following equation

(Fernand et al., 2012):

$$E(r, V) = \frac{V_1 - V_2}{r \ln\left(\frac{R_2}{R_1}\right)} \quad (1)$$

where V_1 is the voltage delivered through the central needle, V_2 is the voltage at the external ring, r is the radial distance of each point inside the treatment area from the center, R_1 is the radius of the needle, and R_2 is the external ring radius.

Pulsed Electric Fields Disinfection of a Prolene Mesh

Regarding the experimental set-up of concentric ring electroporation, a one-dimensional cylindrical system was used, with the diameter of the inner cylinder, represented by an 18-gauge steel needle, measuring 1 mm, and the outer cylinder measuring 22 mm in diameter. The needle was inserted through the center of the plastic in the middle of the brass ring forming two concentric cylindrical electrodes. Alligator clips were attached to the brass ring and the 18G needle. The system was placed on the mesh with the needle located at the center of the mesh. The clips were hooked up to the BTX 830 pulse generator (Fig. 1a and b) (Harvard Apparatus, Inc., Holliston, MA). The PEF parameters tested were: 1500 V (V_1), 0 V (V_2); 100, 150, and 300 pulses, at 50 μ s pulse length duration and 2 Hz frequency. Three pieces of mesh were treated per group for a total of nine pieces of mesh.

Pseudomonas aeruginosa Survival Detection with Bioluminescent Imaging

The bioluminescent imaging system (Hamamatsu Photonics KK, Bridgewater, NJ) consisted of an intensified charge-coupled-device

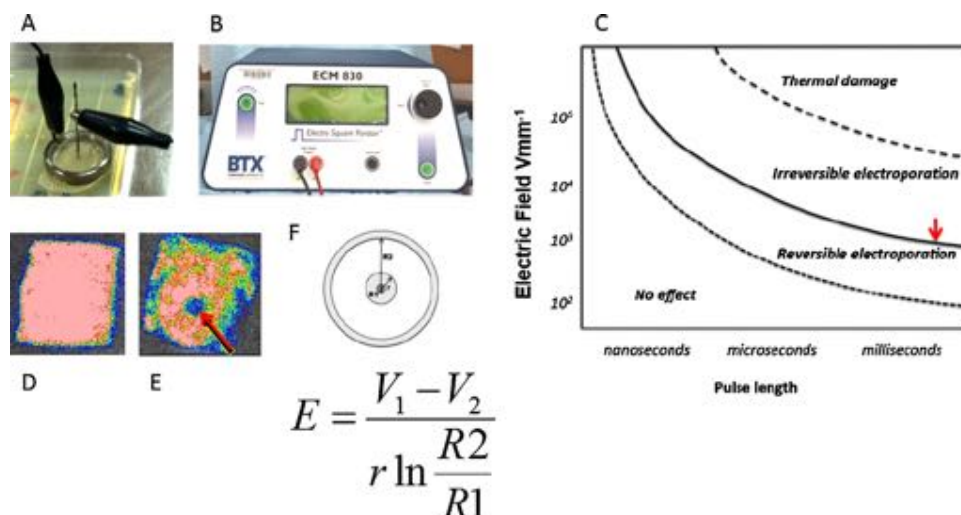


Figure 1. Depiction of experimental setup. (A) Digital image of concentric ring electrodes applied to infected mesh. (B) BTX 830 pulse generator. (C) Theoretical mapping of biophysical effects experienced by cells as a function of electroporation parameters. Our goal was to find the electric field that corresponds to the solid line (red arrow). This represents the minimal electric field needed to kill bacteria and disrupt biofilm. We used the equation displayed to solve for E . (D) Bioluminescent image of infected mesh prior to treatment. (E) Bioluminescent image of infected mesh after treatment where biofilm had been eradicated. (F) Mathematical model of the PEF treatment.

camera mounted in a light-tight specimen chamber fitted with a light-emitting diode. In the photon-counting mode, an image of the light emitted from the bacteria is captured by using an integration time of 2 min at a maximum setting on the image-intensifier control module. Through the use of ARGUS software (Hamamatsu), the luminescent image is presented as a false-color image superimposed on a grayscale reference image. The image-processing component of the software calculates the total pixel values (in Relative Luminescence Units [RLU]) of the infected mesh area. Imaging was performed before treatment with PEF, and immediately after treatment. The percentage of eradicated bacteria can be determined by the intensity of the bioluminescent images (Hamblin et al., 2002). The correlation between bioluminescence and bacterial eradication has been described in previous studies (Ragas et al., 2010; Vecchio et al., 2013) by correlating the CFU and RLU in agar plates in dark control and after treatment with photodynamic therapy.

Scanning Electron Microscopy

Sterile uninfected mesh, untreated infected mesh, and treated infected mesh were processed for Scanning Electron Microscopy (SEM). Samples were placed in ½ strength Karnovsky's fixative immediately after treatment and imaging. Samples remained in fixative for 24 h prior to embedding.

After fixing the samples for 24 h, they were dehydrated in a series of graded ethanol concentrations. A Tousimis Samdri semi automatic Critical Point Dryer was used to completely dehydrate the samples. The mesh was then mounted on aluminum stubs and coated with Chromium with a GATAN 610 Ion Beam Coater. Samples were then viewed in the SEM at a voltage of 5 kV. For image scanning, a JEOL 7401F Field Emission Scanning Electron Microscope was used. Magnification of images ranged from 25× to 10000×. One to three fields were obtained at each magnification.

Data Analysis

For data analysis, a previously described method involving Matlab SW was used (Blumrosen et al., 2014). A set of images before and after the treatment were used to derive the parameters. First, the luminescence intensity was normalized to the correct value to compensate for the difference in the microscope settings before and after the scanning according to (Dai et al., 2010). Following the normalization, the pixels were converted to distances, where each pixel length was 5 mm. The intensity as a function of radius r , for each exposure time t , $I_t(r)$, was obtained by calculating the average intensity of a cluster of bacteria according to the following:

$$I_t(r) = \frac{1}{N_r} \sum_{r-\delta \leq r' \leq r+\delta} I_t(r') \quad (2)$$

where $r = \sqrt{(x - x_{ct})^2 + (y - y_{ct})^2}$ represents the spherical radius from the center of the plate (x_{ct} , y_{ct}), (x, y) are the coordinates of the plate, δ is the length of the cluster in mm, and N_r is the normalization factor, which refers to the number of pixels in

the cluster in the spherical radius. The intensity over different distances, $I_t(r)$, was converted to intensity over electrical field strength using Equation (1).

The relationship between the survival fraction and the treatment time (for a pre-determined pulse energy) is commonly described by a mathematical model based on the Weibull distribution (Álvarez et al., 2003; Peleg and Pechina, 2000; Peleg and Cole, 2000):

$$\log S = -\frac{1}{2.303} \left(\frac{E}{b}\right)^n \quad (3)$$

where S is the survival fraction of bacteria after the treatment, E is the local electric field, and b and n are the field normalization and field exponent factors that can be estimated from fitting the empirical data for each pulse rate. The fitting we used to estimate these parameters was least-squares nonlinear curve-fitting. The Weibull distribution depicts the dependence of bacterial survival on electric field intensity. We used a medium-scale Quasi-Newton line search for the fitting algorithm (Murtagh and Saunders, 1978).

Results

Quantification of Treatment Efficacy Dependence on Pulse Rate and Electrical Field Strength

To quantify the effect of pulse number using 100, 150, and 300 pulses, where the voltage, pulse length duration, and frequency remained unchanged (1500 V, 50 μs, and 2 Hz, respectively), we analyzed the images before and after treatment with concentric ring electrodes. The effect of treatment was measured as a function of the radius of central clearing as seen in the bioluminescent images of the mesh.

Figure 2 shows images of the mesh before and after treatment with concentric ring electrodes. It is seen that in all treatments with 150 and 300 pulses there is an effect that results in lower intensity in the images after treatment. To quantify the treatment effect we define effective eradicated area where there is over 80% eradication. According to this criterion, the critical electrical field strength was 121 ± 14 V/mm when 300 pulses were applied, 235 ± 6.1 V/mm when 150 pulses were applied, with related eradication area of 50.5 ± 9.9 mm² for 300 pulses and 13.4 ± 0.65 mm² for 150 pulses (Table I). This indicates that the treatment efficacy increases as the number of pulses increases. More importantly, a clear increase in treatment efficacy is appreciated at the center of the mesh, which was the area that received the strongest electric field delivery even at 100 pulses (Fig. 3). Here, thick biofilm matrix wedged into interstices was noted in control untreated infected mesh. Dense bacteria were present with a clear production of exopolysaccharide which is associated with biofilm formation. After treatment with PEF even with 100 pulses, the biofilm was disrupted and a layer of debris was left behind at the center of the ring, where the fields were the highest. The few remaining scant rods displayed abnormal morphology and exopolysaccharide was not visible. The mesh was not damaged by PEF treatment (Fig. 3).

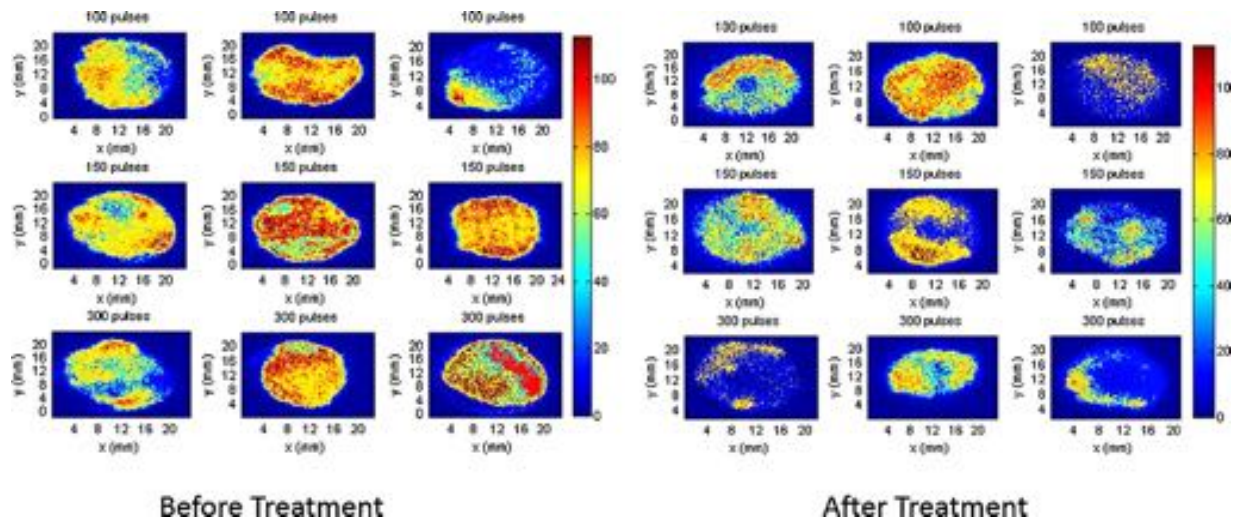


Figure 2. Bioluminescent images of mesh before and after treatment. Bioluminescent images of the infected prolene mesh before and after treatment with concentric ring electrodes. It is seen that in all ($N=3$ treated mesh) 150 and 300 pulses treatments there is an effect that results in lower bioluminescent intensity in the images after treatment.

Survival rate is defined as the ratio of bacterial survival (measured as RLU) compared to the initial value, and is depicted in a logarithmic scale. Figure 4A shows the average of all treatments per pulse group, compared to the theoretical Weibull distribution as a function of the electrical field strength. It can be appreciated from the figure that the survival rate decreases as the number of pulses and electrical field strength increase. However, at the lower pulse rate of 100 pulses, it seems that the effect of the treatment is similar across different electrical field strengths; whereas, at the higher pulse rate of 300 pulses, there is a more dramatic effect at the center of the mesh, where the electrical field strength is highest. An ANOVA test (Fig. 4B) shows that the P -value between the different conditions (pulse number) is 5.6×10^{-5} with error degrees of freedom (df) of 15, which indicates that the increased efficacy of treatment is due to the increased number of pulses delivered. The average values between the conditions were 57.41, 74.35, and 81.11, for the 50, 150, and 300 number of initial pulses, respectively. A multiple comparisons testing (pairwise comparison) using “Tukey–Kramer” criterion that was performed after the Anova, showed the difference between the estimated group means as depicted in Figure 4B. The differences in means between 150 and 300 pulses is -6.7579 , which is significantly lower than the difference in means between 150 and 50, and 300 and 50 (-16.9356 and -23.6935 , respectively). Still, the lower and upper limits for 95% confidence intervals for 150 and 300 pulses, was -12.2820 and -1.2338 , with

P -value of 0.101, which indicates a marginal significance between 150 and 300 pulses. This indicates that the effect of number of pulses between 150 and 300 pulses is considerably small compared to lower pulse numbers. Table I summarizes the treatment efficacy of each of the three groups of pulses.

Comparison of the Treatment Efficacy to a Theoretical Model

The model fitting to the theoretical Weibull distribution in Equation (3), is very high with a correlation coefficient R^2 of 0.9563, 0.9943, and 0.9956, for the 100, 150, and 300 pulses, respectively. The model fitting is more accurate in the case of higher pulses, where the treatment effect is more significant. The model fitting parameters used, and their corresponding R^2 , are shown in Table II.

Discussion

We have demonstrated, *in vitro*, that pulsed electric fields can eradicate bacteria and disrupt biofilms in mesh implants without damaging the mesh. Biofilms are a significant medical problem, causing eighty percent of infections in the body. Examples include infections of indwelling catheters, cardiac implants, prosthetic heart valves, synthetic vascular grafts and stents, internal fixation devices, synthetic mesh, tracheal and ventilator tubing, oral soft tissues, dental implants and teeth, middle ear, gastrointestinal tract, airway/lung tissue, eyes, urogenital tract, urinary tract prostheses, peritoneal membrane and peritoneal dialysis catheters, and percutaneous sutures. Bacteria within biofilms have increased resistance to antibiotics, even though these same bacteria are sensitive to antibiotics if grown under planktonic conditions (2002–12–20). Most recent studies, have shown that extracellular DNA, secreted by bacteria, prevent efficient drug delivery to the biofilms (Baelo et al., 2015).

Table I. Bacterial eradication results for number of pulses delivered ($V_1 = 1500$, $V_2 = 0$, pulses, $50 \mu\text{s}$ pulse length duration, and 2 Hz).

Treatment	E_{cr} for 80% eradication (V/mm)	Area eradicated over 80% (mm^2)
100 pulses	none	none
150 pulses	121 ± 14	50.5 ± 9.9
300 pulses	235 ± 6.1	13.4 ± 0.65

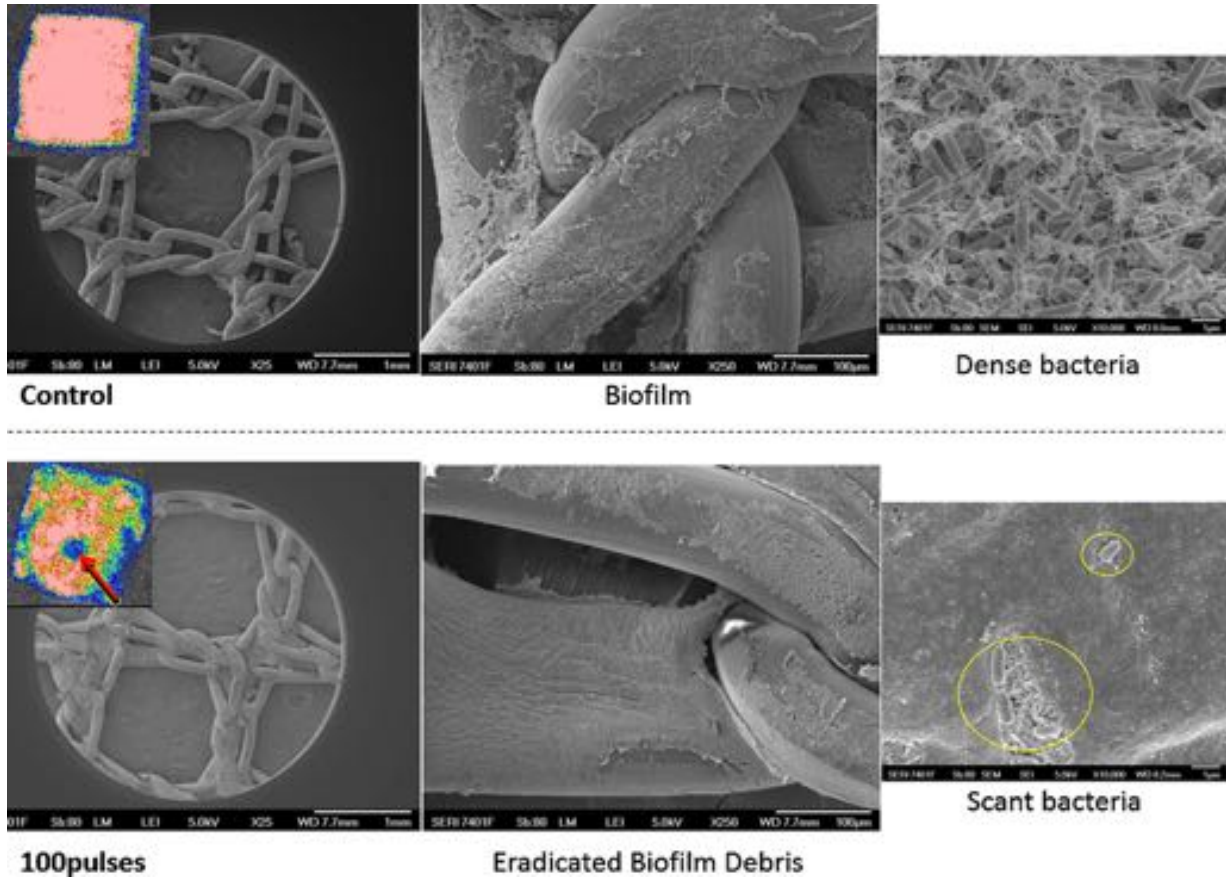


Figure 3. Scanning Electron Microscopy confirmed our results. Control untreated infected mesh demonstrated thick biofilm wedged into mesh interstices. Dense bacteria revealed production of exopolysaccharide. After treatment with PEF using the concentric electrodes, the biofilm has been disrupted and debris is left behind. The few remaining scant rods displayed abnormal morphology and exopolysaccharide was not visible. The mesh was not damaged by PEF treatment.

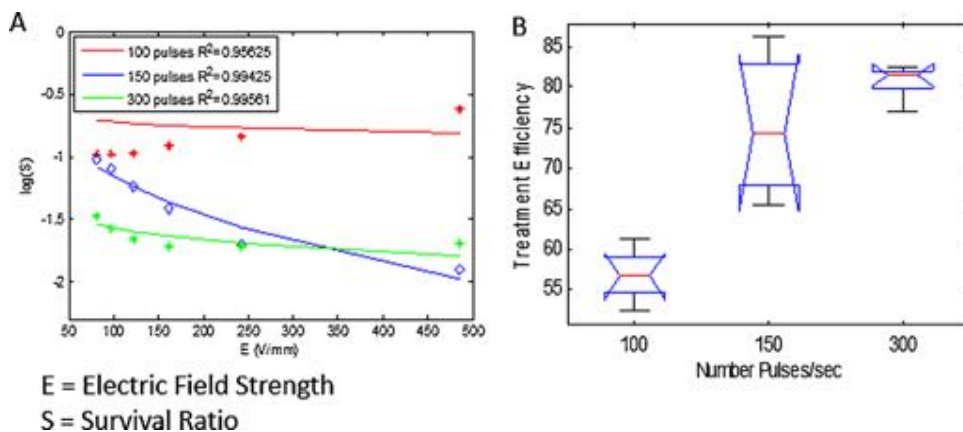


Figure 4. Log (Survival Ratio) of bacteria per treatment group. **(A)** Bioluminescent values measured from $N=3$ mesh pieces per group. The average of all treatments per pulse group compared to the theoretical Weibull distribution as a function of the electric field strength, is demonstrated. Survival rate decreases as the number of pulses and electric field strength increase. **(B)** An ANOVA test reveals that the P -value between the different conditions (pulse number) is 0.000056, which indicates that treatment efficacy directly correlates to number of pulses delivered. Treatment efficiency is defined by the % of eradicated bacteria, as measured by the % of bioluminescence reduction at the specific location.

Table II. Fitting results to the theoretical model.

Treatment	(b,n)	R ²
100 pulses	-0.49, 0.074	0.9563
150 pulses	5.4650, 0.3379	0.9943
300 pulses	0.0001, 0.0828	0.9956

In this study, we demonstrated the effectiveness of PEF treatment of biofilm-infected mesh. The results show increased bacterial eradication with increased number of pulses, and electrical field strength. Additionally, the area of complete eradication of bacteria increases as the number of pulses increases ($P = 0.000056$). This indicates that increased efficacy of treatment is due to increased number of pulses delivered. Additionally, the P -value between the conditions of 150 and 300 pulses was 0.101, which indicates a marginal significance between 150 and 300 pulses. This indicates that the effect of number of pulses between 150 and 300 pulses is considerably small compared to lower pulse numbers (50), where the effect on survival rate is less. Thus, for future treatments, less than 300 pulses can be chosen, without significant impact on treatment efficiency. In addition, we showed that the results of this work are consistent with the theoretical Weibull model. Study limitations include the fact that this is an in vitro model and only one type of synthetic implant was tested. In addition, we did not test the effects of pulse length duration on efficacy of treatment, nor combine this treatment with antibiotics. The depth of PEF treatment can be controlled in order to avoid damage to surrounding tissue and/or organs if clinically applied in a patient with infected mesh (Golberg and Rubinsky, 2012). The treated area in the clinical scenario will be predefined by the configuration of the electrodes and the applied PEF parameters. Our previous work showed that PEF-ablated skin heals with no evidence of scarring (Golberg and Yarmush, 2013). In order for the effect of PEF treatment to be maximized, it would work synergistically with the human immune system and IV antibiotics. PEF will stimulate the immune system by recruiting inflammatory cytokines and mediators to the site of treatment (Golberg et al., 2015), and it has the potential to eradicate the biofilm synergistically with antibiotics. Disruption of bacteria in the biofilm could decrease the concentration of secreted molecules such as eDNA in the biofilm, therefore, enabling more efficient drug delivery to the treated area. This hypothesis should be evaluated in vivo in an animal model, as well as clinical trials. We do not know the long-term response of the body to an infected material treated by PEF.

In conclusion, PEF treatment avoids the problem of antibiotic resistance. Additionally, PEF does not involve enzymatic removal (Johansen et al., 1997), chemical treatments (Chen, 2000), metallic nanoparticles (Chen et al., 2014), chelating agents (Turakhia et al., 1983), or other methods previously applied to biofilms. Moreover, PEF is a non-thermal treatment that does not destroy the integrity of the mesh or damage the mesh at all, while sparing surrounding tissue from injury. Combining antibiotic therapy with PEF could effectively eradicate biofilms, therefore, avoiding mesh removal and/or life-long high-dose antibiotic therapy. In the future, we plan to test this treatment in an in vivo model. We have established the parameters needed to achieve

complete bacterial eradication with a single needle electrode. Based on the results of this study, a tailored device could be created with an array of needles at various distances apart from each other to treat any given infected mesh in a patient.

We thank Ann Tisdale, an expert at The Schepens Eye Research Institute, Massachusetts Eye and Ear SEM Core Facility, for her valuable Scanning Electron Microscopy knowledge, skill, and contributions. DV and MRH were supported by US NIH grant R01AI050875.

References

- Álvarez I, Raso J, Sala F, Condón S. 2003. Inactivation of *Yersinia enterocolitica* by pulsed electric fields. *Food microbiol* 20:691–700.
- Albino FP, Patel KM, Nahabedian MY, Attinger CE, Bhanot P. 2014. Immediate, multistaged approach to infected synthetic mesh: Outcomes after abdominal wall reconstruction with porcine acellular dermal matrix. *Ann Plast Surg* DOI: 10.1097/SAP000000000000186.
- Baelo A, Levato R, Julian E, Crespo A, Astola J, Gavalda J, Engel E, Mateos-Timoneda MA, Torrents E. 2015. Disassembling bacterial extracellular matrix with DNase-coated nanoparticles to enhance antibiotic delivery in biofilm infections. *J Control Release* 209:150–158.
- Bjarnsholt T. 2013. The role of bacterial biofilms in chronic infections. *APMIS Suppl* 1–51.
- Blumrosen G, Abazari A, Golberg A, Tonner M, Yarmush ML. 2014. Efficient Procedure and Methods to Determine Critical Electroporation Parameters. Paper presented at: Proceedings of the 2014 IEEE 27th International Symposium on Computer-Based Medical Systems (IEEE Computer Society).
- Breuing K, Butler CE, Ferzoco S, Franz M, Hultman CS, Kilbridge JE, Rosen M, Silverman RP, Vargo D. 2010. Incisional ventral hernias: Review of the literature and recommendations regarding the grading and technique of repair. *Surgery* 148:544–558.
- Chen CW, Hsu CY, Lai SM, Syu WJ, Wang TY, Lai PS. 2014. Metal nanobullets for multidrug resistant bacteria and biofilms. *Adv Drug Deliv Rev* 78:88–104.
- Chen XS. 2000. Biofilm removal caused by chemical treatments. *Water Res* 34:4229–4233.
- Costerton JW, Lewandowski Z, Caldwell DE, Korber DR, Lappin-Scott HM. 1995. Annual review of microbiology. *Microbial Biofilms* 49:711–745.
- Dai T, Tegos GP, Zhiyentayev T, Mylonakis E, Hamblin MR. 2010. Photodynamic therapy for methicillin-resistant *Staphylococcus aureus* infection in a mouse skin abrasion model. *Lasers Surg Med* 42:38–44.
- Davies DG, Marques CN. 2009. A fatty acid messenger is responsible for inducing dispersion in microbial biofilms. *J Bacteriol* 191:1393–1403.
- Fernand F, Rubinsky L, Golberg A, Rubinsky B. 2012. Variable electric fields for high throughput electroporation protocol design in curvilinear coordinates. *Biotechnol Bioeng* 109:2168–2171.
- Golberg A, Rubinsky B. 2012. Towards electroporation based treatment planning considering electric field induced muscle contractions. *Technol Cancer Res Treat* 11:189–201.
- Golberg A, Yarmush ML. 2013. Nonthermal irreversible electroporation: fundamentals, applications, and challenges. *IEEE Trans Biomed Eng* 60:707–714.
- Golberg A, Fischer J, Rubinsky B. 2010. The Use of Irreversible Electroporation in Food Preservation. In *Irreversible Electroporation*. Berlin Heidelberg: Springer. p 273–312.
- Golberg A, Broelsch GF, Vecchio D, Khan S, Hamblin MR, Austen WG, Jr, Sheridan RL, Yarmush ML. 2014a. Eradication of multidrug-resistant in burn wounds by antiseptic pulsed electric field. *Technology* 2:153–160.
- Golberg A, Broelsch GF, Vecchio D, Khan S, Hamblin MR, Austen WG, Jr, Sheridan RL, Yarmush ML. 2015b. Pulsed Electric Fields for Burn Wound Disinfection in a Murine Model. *J Burn Care Res* 36(1):7–13.
- Golberg A, Khan S, Belov V, Quinn KP, Albadawi H, Broelsch GF, Watkins MT, Georgakoudi I, Papisov M, Mihm MC, Jr. 2015b. Skin rejuvenation with pulsed electric fields. *Scientific Reports* 5:10187.
- Golberg AY, M L. 2013. Nonthermal irreversible electroporation: Fundamentals, applications, and challenges. *IEEE Trans Biomed Eng* 60:707–714.

- Golberg A. 2015. Long-term *Listeria monocytogenes* proliferation control in milk by intermittently delivered pulsed electric fields, implications for food security in the low-income countries. *Technology* 3:1–6.
- Hamblin MR, O'Donnell DA, Murthy N, Contag CH, Hasan T. 2002. Rapid control of wound infections by targeted photodynamic therapy monitored by in vivo bioluminescence imaging. *Photochem Photobiol* 75:51–57.
- Hoiby N, Bjarnsholt T, Givskov M, Molin S, Ciofu O. 2010. Antibiotic resistance of bacterial biofilms. *Int J Antimicrob Agents* 35:322–332.
- Johansen C, Falholt P, Gram L. 1997. Enzymatic removal and disinfection of bacterial biofilms. *Appl Environ Microbiol* 63:3724–3728.
- Jolivet-Gougeon A, Kovacs B, Le Gall-David S, Le Bars H, Bousarghin L, Bonneure-Mallet M, Lobel B, Guille F, Soussy CJ, Tenke P. 2011. Bacterial hypermutation: Clinical implications. *J Med Microbiol* 60:563–573.
- Manca G, Pandolfi P, Gregorelli C, Cadossi M, de Terlizzi F. 2013. Treatment of keloids and hypertrophic scars with bleomycin and electroporation. *Plast Reconstr Surg* 132:621e–630e.
- Markley K, Smallman E. 1968. Protection by vaccination against *Pseudomonas* infection after thermal injury. *J Bacteriol* 96:867–874.
- Mir LM, Gehl J, Sersa G, Collins CG, Garbay J-R, Billard V, Geertsen PF, O'Sullivan GC, M. 2006. Standard operating procedures of the electrochemotherapy: Instructions for the use of bleomycin or cisplatin administered either systemically or locally and electric pulses delivered by the Cliniporator™ by means of invasive or non-invasive electrodes. *Eur J Cancer* 4:14–25.
- Murtagh BA, Saunders MA. 1978. Large-scale linearly constrained optimization. *Mathematical Programming* 14:41–72.
- Neal RE, 2nd, JH Rossmeisl, Jr, Garcia PA, Lanz OI, Henao-Guerrero N, RV Davalos. 2011. Successful treatment of a large soft tissue sarcoma with irreversible electroporation. *J Clin Oncol* 29:e372–e377.
- Peleg M, Cole MB. 2000. Estimating the survival of *Clostridium botulinum* spores during heat treatments. *J Food Prot* 63:190–195.
- Peleg M, Penchina CM. 2000. Modeling microbial survival during exposure to a lethal agent with varying intensity. *Crit Rev Food Sci Nut* 40:159–172.
- Ragas X, Dai T, Tegos GP, Agut M, Nonell S, Hamblin MR. 2010. Photodynamic inactivation of *Acinetobacter baumannii* using phenothiazinium dyes: in vitro and in vivo studies. *Lasers Surg Med* 42:384–390.
- Rocchetta HL, Boylan CJ, Foley JW, Iversen PW, LeTourneau DL, McMillian CL, Contag PR, Jenkins DE, Parr TR. 2001. Validation of a noninvasive, real-time imaging technology using bioluminescent *Escherichia coli* in the neutropenic mouse thigh model of infection. *Antimicrob Agents Chemother* 45:129–137.
- Rosenthal S. 1967. Local and systemic therapy of *Pseudomonas septicemia* in burned mice. *Ann Surg* 165:97–103.
- Sandt C, Smith-Palmer T, Pink J, Brennan L, Pink D. 2007. Confocal Raman microspectroscopy as a tool for studying the chemical heterogeneities of biofilms in situ. *J Appl Microbiol* 103:1808–1820.
- Sersa G, Jarm T, Kotnik T, Coer A, Podkrajsek M, Sentjurc M, Miklavcic D, Kadivec M, Kranjc S, Secerov A. 2008. Vascular disrupting action of electroporation and electrochemotherapy with bleomycin in murine sarcoma. *Br J Cancer* 98:388–398.
- Turakhia MH, Cooksey KE, Characklis WG. 1983. Influence of a calcium-specific chelant on biofilm removal. *Appl Environ Microbiol* 46:1236–1238.
- Vecchio D, Dai T, Huang L, Fantetti L, Roncucci G, Hamblin M. 2013. Antimicrobial photodynamic therapy with RLP068 kills methicillin-resistant *Staphylococcus aureus* and improves wound healing in a mouse model of infected skin abrasion PDT with RLP068/Cl in infected mouse skin abrasion. *J Biophotonics* 6:733–742.
- Weaver JC. 2000. Electroporation of cells and tissues. *IEEE Trans Plasma Sci* 28:24–33.
- Xavier JB, Picioreanu C, Rani SA, van Loosdrecht MC, Stewart PS. 2005. Biofilm-control strategies based on enzymic disruption of the extracellular polymeric substance matrix—a modelling study. *Microbiology* 151:3817–3832.
- Yarmush ML, Golberg A, Sersa G, Kotnik T, Miklavcic D. 2014. Electroporation-based technologies for medicine: Principles, applications, and challenges. *Annu Rev Biomed Eng* 16:295–320.